

Article

State of Charge Estimation of a Lithium Ion Battery Based on Adaptive Kalman Filter Method for an Equivalent Circuit Model

Xiao Ma , Danfeng Qiu *, Qing Tao and Daiyin Zhu

Key Laboratory of Radar Imaging and Microwave Photonics (Nanjing University of Aeronautics and Astronautics), Ministry of Education, College of Electronic and Information Engineering, Nanjing University of Aeronautics and Astronautics, Nanjing 211100, China

* Correspondence: dfqiu@nuaa.edu.cn

Received: 30 April 2019; Accepted: 4 July 2019; Published: 9 July 2019



Abstract: Due to its accuracy, simplicity, and other advantages, the Kalman filter method is one of the common algorithms to estimate the state-of-charge (SOC) of batteries. However, this method still has its shortcomings. The Kalman filter method is an algorithm designed for linear systems and requires precise mathematical models. Lithium-ion batteries are not linear systems, so the establishment of the battery equivalent circuit model (ECM) is necessary for SOC estimation. In this paper, an adaptive Kalman filter method and the battery Thevenin equivalent circuit are combined to estimate the SOC of an electric vehicle power battery dynamically. Firstly, the equivalent circuit model is studied, and the battery model suitable for SOC estimation is established. Then, the parameters of the corresponding battery charge and the discharge experimental detection model are designed. Finally, the adaptive Kalman filter method is applied to the model in the unknown interference noise environment and is also adopted to estimate the SOC of the battery online. The simulation results show that the proposed method can correct the SOC estimation error caused by the model error in real time. The estimation accuracy of the proposed method is higher than that of the Kalman filter method. The adaptive Kalman filter method also has a correction effect on the initial value error, which is suitable for online SOC estimation of power batteries. The experiment under the BBDST (Beijing Bus Dynamic Stress Test) working condition fully proves that the proposed SOC estimation algorithm can hold the satisfactory accuracy even in complex situations.

Keywords: SOC; adaptive Kalman filter; equivalent circuit model

1. Introduction

Due to the global energy shortage and environmental pollution, countries around the world have attached great importance to the development of electric vehicles. The lithium-ion battery is considered to be an ideal electric vehicle power battery with high safety, large discharge power, environmental protection, less pollution, and long cycle life [1,2]. However, the increase in energy density and electrochemical performance of the battery often means a decrease in safety performance, which is prone to safety accidents. In the process of use, because of the side reaction of the electrolyte and the interface between the positive and negative electrodes, the thermal and electrical properties of the aged lithium-ion battery will be significantly changed and, therefore, the thermal stability of the lithium-ion battery will inevitably change as it ages [3]. In [4], the differences in the safety behavior between un-aged and aged high-power 18650 lithium-ion cells were investigated at the cell and material level by accelerating rate calorimetry (ARC) and simultaneous thermal analysis (STA). The results show that the aging of the battery will lead to the mechanical deformation of the jelly roll and lithium plating

on the anode, which has a great impact on battery safety. The cyclic stability and thermal runaway characteristics of four commercially available cylindrical batteries under three different states-of-charge (0, 50%, and 100%) were investigated in [5]. Abuse testing (crush and nail penetration tests) was also performed at 100% SOC. It is not difficult to see from the analysis of the article that the SOC of the battery is related to the thermal stability of the battery. The higher the SOC, the worse the thermal stability of the battery, and the lower the temperature of the thermal runaway.

In actual practice, lithium-ion batteries need to be well monitored, judged, and controlled by the battery management system (BMS). An accurate battery state estimation is one of the most basic functions of the BMS. The state of the battery includes state-of-charge (SOC), state-of-health (SOH), and state-of-function (SOF). SOC refers to the battery's remaining capacity and is one of the main parameters describing the state of the battery. An accurate estimation of the SOC can effectively prevent battery overcharge and over discharge, extend battery life, and provide drivers with accurate cruising range information. SOC of the battery cannot be directly measured by the instrument and can only be estimated from other measurable parameters. However, external factors and internal factors, such as ambient temperature, self-discharge, and cycle life, can affect the estimation of the battery's SOC. How to accurately estimate the battery capacity is a worldwide problem.

With the development of technology, a series of battery SOC estimation algorithms have been proposed; each has its advantages and disadvantages. The common battery SOC estimation methods include: (1) the residual capacity method [6]; (2) the open circuit voltage (OCV) method [7]; (3) the ampere-hour integration method [8]; (4) the Kalman filter method [9]; (5) the deep learning algorithm [10]; (6) the neural network method [11]; and (7) hybrid techniques [9].

The residual capacity method calculates the SOC by discharging the battery to a lower cut-off voltage in the controlled test equipment [6] and the OCV method is based on the relationship between the open circuit voltage of the battery and the SOC [7]. The results obtained by the two methods in the laboratory are very reliable, but both require a large amount of measurement time and are not suitable for online monitoring of the BMS. The ampere-hour integration method estimates the SOC by integrating the inflow and outflow currents of the battery. The method is easily calculated online and the cost is low. However, this method cannot correct the cumulative error caused by the drift of the current measurement sensor. In addition, the accuracy of the estimation depends on the initial SOC [8]. This method has low robustness against the acquired signal quality and the initial SOC.

The neural network method and the deep learning method can be referred to as machine learning methods. These methods do not require detailed information on the battery system, also known as the "black box" model. Chaoran Li et al. designed a SOC estimation method based on the recurrent neural network (RNN) [12]. Observable variables, such as voltage, current, and temperature, are directly mapped to SOC estimates. Experimental results show that the method is accurate and robust. Phattara Khumprom et al. described a method for predicting state-of-health (SOH) and remaining useful life (RUL) of the battery based on deep learning [10]. Although there have been many studies on machine learning methods and many of them have shown very good performance, these methods still have shortcomings. The computational burden is heavy and poses a serious challenge to the performance of the BMS. Moreover, the cost of implementing these methods is very high and the practicality is still relatively poor. Although the practicality is not strong at present, more and more people have begun to explore ways to estimate SOC by better machine learning methods.

The hybrid technique means an SOC estimation method that combines various SOC estimation methods appropriately. For example, Liu et al. designed an SOC estimation method combining the adaptive extended Kalman filter method (AEKF) and the ampere-hour integration method together [9]. The experimental results show that the accuracy of this method is relatively high and the calculation time is short, and the practicability is better. The greatest problem with this method at present is that the cost of computing is still very high. Still with the article of Liu as an example [9], the method proposed in this paper needs to construct the adaptive extended Kalman filter method and the ampere-time

integral method at the same time, which undoubtedly brings a great burden to the BMS. However, finding the right hybrid method is still one of the development directions for the future SOC estimation.

Compared with the above methods, the Kalman filter method is more accurate and easier to implement. The Kalman filter method does not require an accurate SOC initial value because the result will gradually approach the optimal value and the current measurement error will update the algorithm during operation. At the same time, it is a closed-loop observer that achieves the accurate and continuous estimation of performance over the entire battery operating range. The above advantages make the Kalman filter a promising solution to BMS application implementation. The traditional Kalman filter is only applicable to linear systems, while BMS applications require nonlinear algorithms for more complex systems [13]. Several modifications have been proposed, such as the Extended Kalman Filter (EKF) [14], the Unscented Kalman Filter (UKF) [15], and the Adaptive Kalman Filter (AKF) [16]. Among them, AKF has ability to update the process and measure the noise covariance, which can estimate the SOC more accurately [17].

The most challenging issue in the SOC estimation is the trade-off between balance accuracy and computational cost [9]. In general, the more complex the algorithm, the higher the accuracy, but the higher the cost. According to the authors' knowledge, BMS engineers of electric vehicle manufacturers generally believe that the SOC estimation module can be considered qualified if the error is less than 5%. The cost of the BMS is relatively high, accounting for more than 10% of the cost of the whole vehicle. A more complicated method may increase the accuracy of the SOC to less than 2%, but the cost usually doubles. In summary, modern intelligent algorithms for the BMS for the online SOC estimation require the following features: an accurate description of the battery system under dynamic excitation; an adaptive adjustment of system noise; system stability and robustness; and lower calculation cost. In order to meet these conditions, this paper proposes a method for the online SOC estimation based on the Thevenin equivalent circuit model and the adaptive Kalman filter method. This paper aims to make the following contributions:

- (1) By comparing and analyzing ECMs, the most suitable ECM and parameter identification algorithms are decided;
- (2) A low-cost and accurate SOC estimator based on the adaptive Kalman filter (AKF) for the proposed model is developed, and its accuracy and robustness are verified by experiments under constant current working conditions and BBDST working conditions; and
- (3) The proposed method has strong robustness to model uncertainty and strong mutation to state tracking ability.

The rest of this article is organized as follows: Section 2 describes a practical method for plotting the OCV vs. SOC curve for a battery, identifying the corresponding parameters of the Thevenin equivalent circuit. Section 3 describes the calculation method of the adaptive Kalman filter in detail. The experimental process is described in Section 4 and the experimental results are analyzed. Finally, Section 5 states the conclusions.

2. The Determination of the Battery Model

2.1. The SOC-OCV Relationship Curve

SOC means the residual capacity of the battery, which is a very important parameter for electric vehicles, especially in the operation of electric vehicles, which is particularly important for the correct arrangement of the remaining quantity and time in the course of the travel. Its mathematical expression is $SOC = \frac{Q_r}{Q_N} \times 100\%$. Q_r is the remaining capacity of the battery, and Q_N is the rated quantity of the battery under the same condition. However, since the value of Q_r is difficult to be determined directly, this formula is rarely used in actual calculations. The most commonly used formula to calculate the battery SOC is the ampere-hour integral (AH) formula:

$$SOC = SOC_0 + \frac{1}{Q_N} \int_0^t \eta I dt \quad (1)$$

Among them Q_N is the rated capacity of the battery, and η is an influence factor related to the temperature and the discharge rate of the battery (approximately equal to 1). I is the charge discharge current of the battery. The AH method is simple and easy to make calculations. It only needs to collect the real time current and obtains SOC by integrating the time with the current [18–20].

OCV means the current battery capacity of the battery estimated by measured interruption voltage of the battery in the open circuit state. Since the battery has been static after a long time, its port voltage has a relatively stable function relationship with the SOC, so by OCV, a relatively true SOC estimate can be obtained [21]. Due to the accuracy of the OCV method, the SOC value estimated by this method will be used as the reference value of the proposed method. Therefore, it is necessary to find a method that can accurately find out the relationship between the battery OCV and SOC.

Commercial lithium iron phosphate batteries (LIPB) of 3.2 V/2200 mA_H were used as a research object, and the SOC-OCV relationship curve was measured using the following method (T = 25 °C) [22–24]:

- The battery was discharged to the lower limit voltage;
- The battery was charged to the upper limit voltage with a constant charging current, and the charging voltage and the charging capacity were recorded;
- The battery was discharged at a constant discharge current, and the discharge was stopped when the discharge capacity was the same as the charge capacity in step B, and the discharging voltage and the discharging capacity were recorded; and
- Data of the charging voltage and the discharging voltage of the battery relative to the state of charge of the battery were respectively obtained;

At the same state of charge, the open circuit voltage value took the intermediate value of the charging voltage and the discharging voltage, thereby obtaining a SOC-OCV relationship curve as was shown in Figure 1. A high-order polynomial function representing the OCV-SOC relationship was shown as follows:

$$\begin{aligned}
 OCV = & 4802.561SOC^9 - 22851.658SOC^8 + 46094.256SOC^7 \\
 & - 51274.985SOC^6 + 34272.375SOC^5 - 14077.056SOC^4 \\
 & + 3484.326SOC^3 - 491.298SOC^2 + 35.357SOC + 2.236
 \end{aligned}
 \tag{2}$$

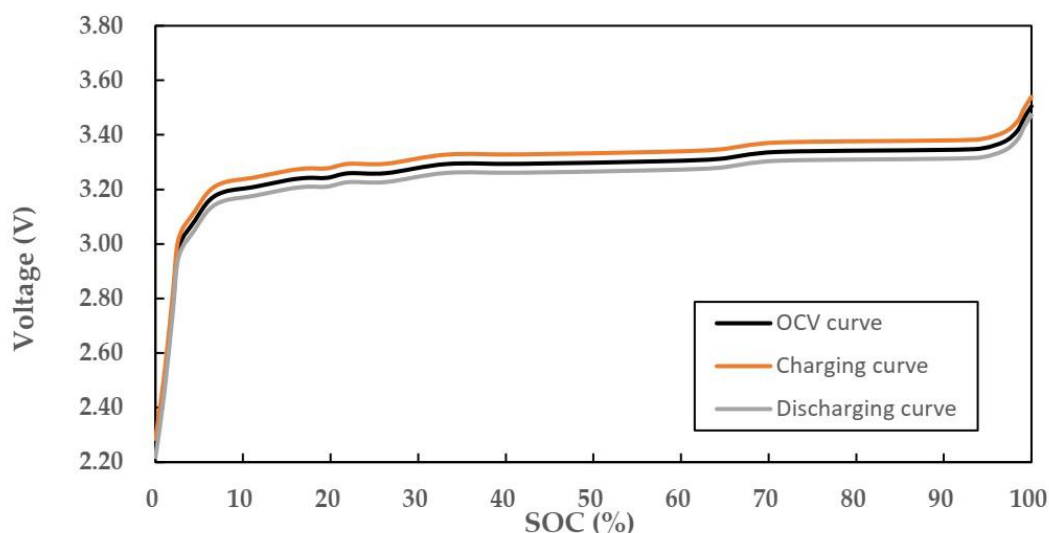


Figure 1. OCV-SOC curve.

2.2. Battery Model Selection and Parameter Identification

The estimation of the adaptive Kalman filter algorithm’s estimation of SOC relies on an accurate and intuitive battery model. In this method, the Thevenin equivalent circuit shown in Figure 2 was used as the estimation model. The Thevenin equivalent circuit, also known as the first-order RC

equivalent model, consists of a voltage source and an RC parallel network. Among them, the parallel circuit composed of R_p and C_p is used to simulate the dynamic response of the battery, which can accurately simulate the charging and discharging process of the battery; U_{oc} is the open circuit voltage of the battery and is positively correlated with the SOC of the battery; R_0 is the resistance characterizing battery characteristics; and U_L is the load voltage of the battery [25–27].

A discretized battery space model is constructed based on the Thevenin equivalent circuit model shown in Figure 2. Among them, the RC network and SOC constructed by R_p and C_p are used as state variables; the charge and discharge current I is used as an input variable, and the output voltage U_L of the battery is used as an output variable. The specific state space model is shown in Equations (3) and (4); Δt is the sampling time interval; $U_p(k)$ is the terminal voltage of capacitance C_p on the k th sampling point; and $SOC(k)$ is the current SOC. And $k-1$ is the sampled value at the previous moment; τ is the time constant of the RC network; η is the coulombic efficiency of charge and discharge; and C_N is the total ampere capacity of the battery [28–30].

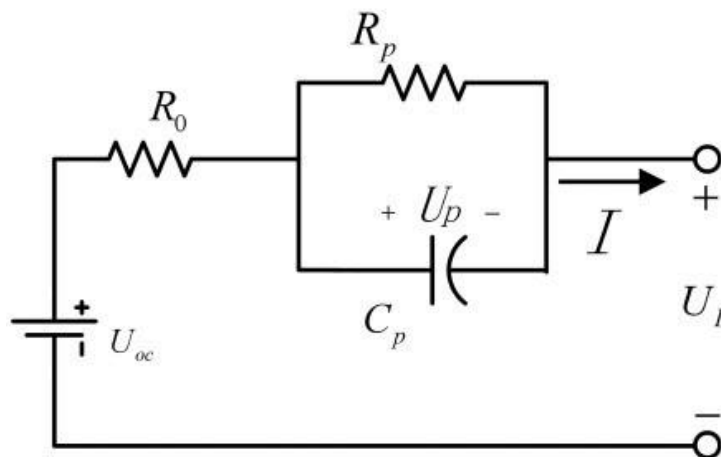


Figure 2. The Thevenin equivalent circuit.

$$\begin{bmatrix} U_p(k) \\ SOC(k) \end{bmatrix} = \begin{bmatrix} R_p(1 - e^{-\frac{\Delta t}{\tau}}) \\ -\frac{\eta \Delta t}{C_N} \end{bmatrix} I(k) + \begin{bmatrix} e^{-\frac{\Delta t}{\tau}} & 0 \\ 0 & 1 \end{bmatrix} \begin{bmatrix} U_p(k-1) \\ SOC(k-1) \end{bmatrix} \quad (3)$$

$$U_L(k) = \begin{bmatrix} -1 & \frac{dU_{oc}(SOC)}{dSOC} \end{bmatrix} \begin{bmatrix} U_p(k) \\ SOC(k) \end{bmatrix} - R_0 I(k) \quad (4)$$

Since OCV and SOC are exponentially corresponding according to Figure 2, the exponential fitting method is adopted to fit the response curve, and then the required model parameters are obtained. The relationship between the discharge current and the output load voltage is obtained by the Thevenin equivalent circuit model:

$$U_L = (U_{oc} - IR_0 - IR_p) + IR_p e^{-\frac{t}{\tau}} \quad (5)$$

An expression is obtained by exponential fitting to Figure 2.

$$U_L = c_1 + c_2 e^{-c_3 t} \quad (6)$$

Among them, c_1 , c_2 , and c_3 are constants, and the circuit model parameters can be obtained by comparing Equations (5) and (6):

$$\begin{cases} R_p = \frac{c_2}{I} \\ C_p = \frac{1}{c_3 R_p} \\ R_0 = (U_{oc} - c_1 - c_2) / I \end{cases} \quad (7)$$

It can be known from Equations (6) and (7), that the parameters of the model components cannot be directly measured, and need to be obtained through identification. There are some standard identification methods and specific processes for the equivalent circuit parameter identification method. According to the HPPC (hybrid pulse power characterization) test method in the *FreedomCAR Battery Test Manual for Power-Assist Hybrid Electric Vehicles*, the experimental data of the lithium-ion battery voltage under constant temperature and different SOC conditions are obtained. The curve is fitted to the obtained data by MATLAB 2014b (The MathWorks, Natick, Massachusetts, USA), and the parameter values under a specific SOC condition at a constant temperature can be identified. The specific steps of the test are described in detail in [31–34]. Table 1 shows the values of the parameters obtained at a temperature of 25 °C.

As can be seen from Figure 1, the SOC value is relatively stable in the range of 0.1–0.9, and changes sharply at both ends. In order to obtain accurate model parameters over the entire interval, multiple data need to be tested in the 0.9–1.0 intervals to ensure that the dramatic changes in the parameters of the interval model can be accurately expressed.

Table 1. Thevenin model identification parameters.

SOC	R ₀ (mΩ)	R _p (mΩ)	C _p (F)
1	33.0	17.2	1987.0
0.975	29.2	16.2	1902.7
0.95	21.6	11.0	1790.7
0.925	19.3	6.5	1881.7
0.9	17.1	7.3	1626.0
0.8	17.1	9.3	1706.9
0.7	17.0	6.1	1702.2
0.6	17.3	5.9	1692.4
0.5	17.6	7.2	1650.3
0.4	17.7	6.2	1274.6
0.3	18.0	6.6	1354.8
0.2	18.4	6.7	1224.6
0.1	18.6	11.4	1135.3

3. The Adaptive SOC Estimation of the Kalman Filter

With the traditional Kalman filter method, it is generally assumed that the interference source is Gaussian white noise when estimating the SOC of the battery is estimated, but in the actual operation of the vehicle, the noise often does not have such good statistical characteristics. Based on this situation, the adaptive Kalman filter algorithm is employed to dynamically estimate the state variables in real time based on the measured data, and to continuously correct the statistical characteristics of the noise, so that the battery SOC can be better approached.

According to Equations (3) and (4), an estimated model of the battery SOC can be obtained:

$$\begin{cases} x_{k+1} = f(x_k, u_k) + \Gamma w_k \\ y_k = g(x_k, u_k) + v_k \\ w_k \sim (q_k, Q_k) \\ v_k \sim (r_k, R_k) \end{cases} \quad (8)$$

In Equation (8), x and y represent state variables and output variables, respectively; Γ is the interference matrix; w_k and v_k are the process noise and measurement noise, which are used to indicate the unknown interference of the battery during operation; q_k , Q_k and r_k , R_k are the corresponding mean and covariance [30].

The steps of estimating the SOC using the adaptive Kalman filter are shown below [35–38]:

1. Initializing the system state gives an estimate of the initial state of the system x_0 and its error covariance P_0 :

$$\widehat{x}_0 = E[x_0] \tag{9}$$

$$P_0 = E[(x_0 - \widehat{x}_0)(x_0 - \widehat{x}_0)^T] \tag{10}$$

2. By iterating the state and the error covariance matrix of the previous moment, the state and error covariance matrix of the next moment can be obtained:

$$\widehat{x}_k = A_k \widehat{x}_{k-1} + B_k u_{k-1} + \Gamma q_{k-1} \tag{11}$$

$$P_k = A_k P_{k-1} A_k^T + \Gamma Q_{k-1} \Gamma^T \tag{12}$$

3. The Kalman gain matrix L_k is:

$$L_k = P_k C_k^T (C_k P_k C_k^T + R_{k-1})^{-1} \tag{13}$$

4. The state error covariance will gradually increase as the uncertainty of the current state increases, resulting in a corresponding increase in the Kalman gain matrix, in order to greatly update the current system state.
5. The state and the state covariance matrix at time k will be updated with output error at time k :

$$\widehat{x}_k = \widehat{x}_{k-1} + L_k (y_k - C_k \widehat{x}_{k-1} - D_k u_k - r_{k-1}) \tag{14}$$

$$P_k = (I - L_k C_k) P_{k-1} \tag{15}$$

6. In Equation (15), I is a unit matrix. As the measured value increases, the stability of the state becomes better and better, so the reference value P_k of uncertainty will be continuously reduced.
7. The mean and the covariance of process noise and measurement noise will be updated:

$$\begin{cases} q_k = (1 - d_{k-1})q_{k-1} + d_{k-1}G(\widehat{x}_k - A_k \widehat{x}_{k-1} - B_k u_{k-1}) \\ Q_k = (1 - d_{k-1})Q_{k-1} + d_{k-1}G(L_k \widetilde{y}_k \widetilde{y}_k^T L_k^T + P_k - A_k P_{k-1} A_k^T)G^T \\ r_k = (1 - d_{k-1})r_{k-1} + d_{k-1}(y_k - C_k \widehat{x}_{k-1} - D_k u_k) \\ R_k = (1 - d_{k-1})R_{k-1} + d_{k-1}(\widetilde{y}_k \widetilde{y}_k^T - C_k P_{k-1} C_k^T) \end{cases} \tag{16}$$

In Equation (16), \widetilde{y}_k is the output error, $\widetilde{y}_k = y_k - C_k x_{k-1} - D_k u_k - r_{k-1}$; $G = (\Gamma^T \Gamma) \Gamma^T$; b ($0 < b < 1$) is the forgetting factor; here take $b = 0.98$. By continuously estimating the mean and the covariance of the noise in real time, the state variable SOC will be continuously updated and the estimation of the SOC will be accurate.

4. Simulation and Results Analysis

4.1. Experiments

Commercial lithium iron phosphate batteries (LIPB) were tested in this study with a nominal voltage of 3.7 V and a nominal capacity of 2200 mAh. The experiment was conducted on a test bench manufactured by Wuhan LANBTS (BT2016C), and the software (Control software client, LANBTS, Wuhan, China) installed on the PC was used to control the charging and discharging of the battery according to the given operating conditions. The terminal voltage and the current of the battery were recorded at a certain frequency. The acquired data is used for model parameter identification and SOC estimation.

Firstly, the SOC and OCV data were obtained using the test bench in conjunction with the experimental method mentioned in Section 2. These data were fitted using MATLAB 2014b (The

MathWorks, Natick, Massachusetts, USA) to obtain OCV-SOC plots and relationships. Secondly, a hybrid pulse power characterization (HPPC) test was performed to identify the parameters of the Thevenin equivalent circuit. The test procedure can be found in the [31–34] and will not be described in detail. Thirdly, a capacity test for finding the standard capacity of the test battery was designed, and its procedures are shown below. Several batteries were placed in a temperature chamber at 25 °C for two hours. Then, the batteries were discharged to 2.2 V at a constant discharge current (1 C). After waiting for two hours, the batteries were fully charged with a constant current. This process would be repeated three times and the average of the test capacity was taken as the standard capacity of the test batteries. Finally, the batteries were respectively tested under the constant current working condition and the Beijing Bus Dynamic Stress Test (BBDST) working condition. Online battery SOC estimation was conducted using the collected data.

4.2. The Comparative Test under Constant Current Discharge Conditions

The battery was discharged at 0.5 C with a simulation duration of 2000 s and a sampling interval of 20 s. The simulation results were shown in Figures 3 and 4. “AKF” stands for the adaptive Kalman filter method; “KF” stands for the Kalman filter SOC estimate. It could be seen from Figures 3 and 4 that the adaptive Kalman filter method was featured with an SOC estimation error of less than 2%, which was higher than the SOC estimation accuracy of the Kalman filter method. Additionally, as can be seen from the figures, the AKF method tends to be stable at about 300 s while the KF method needs about 1100 s. This proves that the AKF method converges quickly, which is very important in practical applications. Therefore, the adaptive Kalman filter method could effectively reduce the influence of unknown noise on SOC estimation.

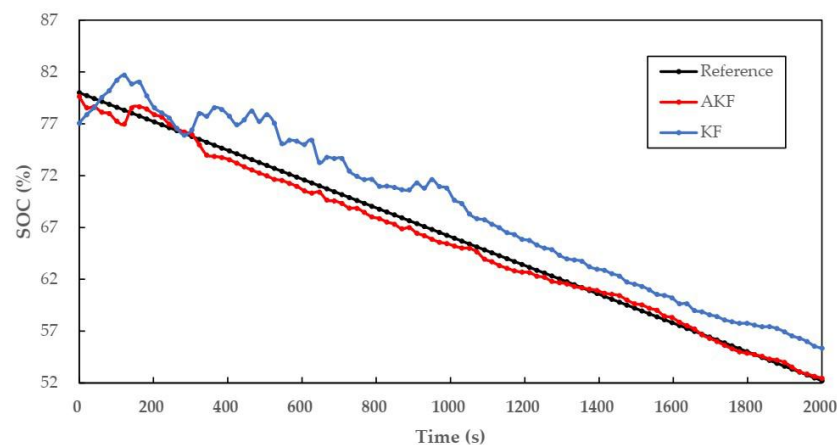


Figure 3. The estimate of SOC using methods of AH, AKF, and KF.

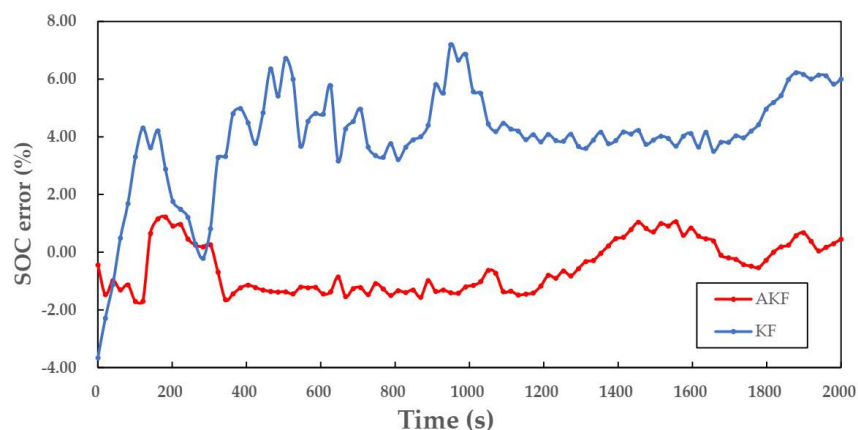


Figure 4. The error of SOC estimate using methods of AH, AKF, and KF.

4.3. The Comparative Test for Initial Value Correction

As can be seen from Figure 1, the OCV value is relatively stable in SOC range of 10–90%. There was a certain error in the initial value of SOC obtained according to the open circuit voltage. Therefore, it was necessary to correct the initial value to reduce the impact of the initial value error on the SOC estimation. In order to verify the correction effect of the adaptive Kalman filter, according to the above method, when the SOC = 0.8, the initial values of the SOC were chosen as 0.76 and 0.81, respectively, and the simulation results are shown in Figures 5 and 6.

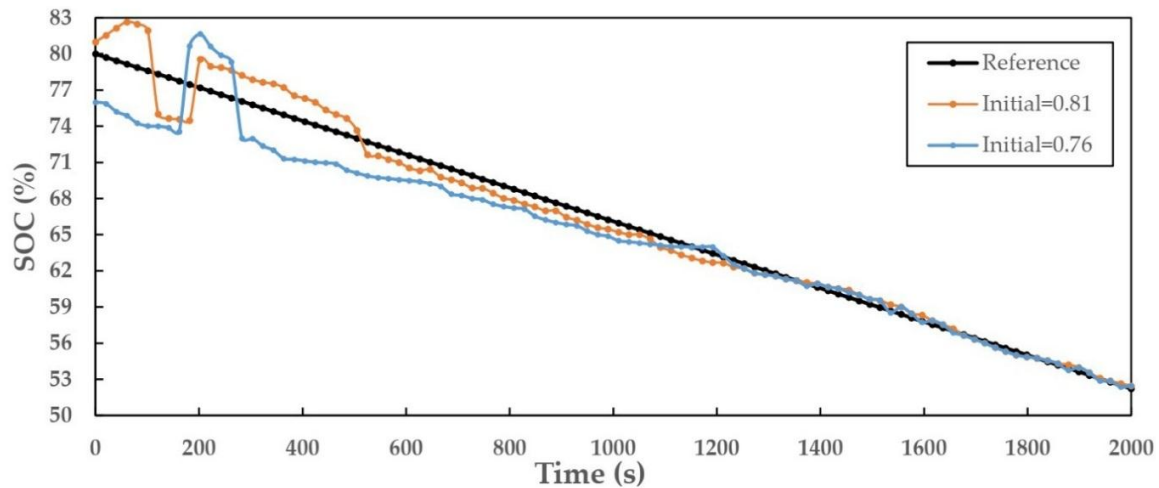


Figure 5. The estimated value of the Kalman filter method when the initial SOC values are different.

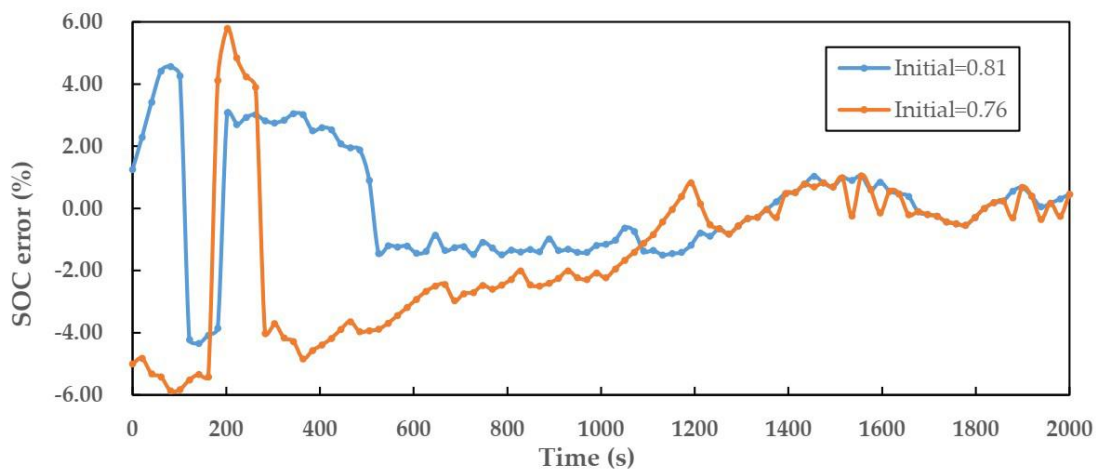


Figure 6. The estimated value error of the Kalman filter method when the initial SOC values are different.

It can be seen from Figures 5 and 6 that, although there is an error in the initial SOC estimation value, the SOC estimation value of the adaptive Kalman filter algorithm converged to be consistent with the actual value (when $-4.00\% \leq \text{error} \leq 4.00\%$) after a short time (no more than 500 s), which fully indicated that the adaptive Kalman filter method had a correction for the initial value error. Moreover, the more accurate the initial value is, the faster the convergence.

4.4. The Simulation Experiment Based on the BBDST Working Condition

The BBDST (Beijing Bus Dynamic Stress Test) working condition is a standard working condition for lithium-ion batteries in China when a 14-day follow-up test of an electric bus on Route 121 in Beijing is conducted, and a condition for simulating the power battery for the vehicle is also obtained. This working condition reflects the SOC change of the electric vehicle battery more than the constant

current working condition. Table 2 shows a detailed step for the entire complete BBDST condition. The total time from the start of the bus to the last stop was 300 seconds [39].

Table 2. The BBDST working condition.

Working Condition	Step Time (s)	Cumulative Time (s)	Battery Output Power (kW)
Start	21	21	37.5
Accelerating	12	33	72.5
Coastdown	16	49	4.5
Brake	6	55	−15
Accelerating	21	76	37.5
Coastdown	16	92	4.5
Brake	6	98	−15
Accelerating	9	107	72.5
Rapid acceleration	6	113	92.5
Uniform speed	21	134	37.5
Coastdown	16	150	4.5
Brake	6	156	−15
Accelerating	9	165	72.5
Rapid acceleration	6	171	92.5
Uniform speed	21	192	37.5
Coastdown	16	208	4.5
Brake	9	217	−35
Brake	12	229	−15
Parking	71	300	4.5

This article used the LANBTS battery test system platform for the BBDST experiments. The SOC interval selected the platform area of 0.1–0.9. Since the experimental equipment was a single battery, the power output from the lithium-ion battery should be adjusted in proportion according to the output power in the standard BBDST operating condition. After conversion, we finally set the ratio of the output power of the lithium-ion battery to the output power of the standard BBDST condition to 1:5000. The specific experimental methods were as follows [39]:

1. Charged the battery to the cut-off voltage at a temperature of 25 °C.
2. After that, it was discharged with a constant current rate of 1 C to SOC = 0.9, and then allowed to stand for 1 h.
3. Performed a complete BBDST test on the lithium-ion battery, then stopped the loading power, and continued to test the lithium-ion battery for a complete BBDST condition after 10 min of static. The above test steps were repeated for achieving 15 complete BBDST condition test cycles.
4. Re-discharged the battery at the 1 C rate until the battery was discharged to the cut-off voltage, finally terminated the discharge, and recorded the experimental data.

Superimposed random noise processing was performed on the current and voltage data obtained by the test. The SOC accurate value was obtained by the OCV method and the ampere-hour method before the superimposed noise was taken as a comparison value of the SOC estimation. The superimposed noise data was substituted into the SOC estimation program designed above for simulation calculation. Finally, the following two figures could be drawn. It can be seen from Figures 7 and 8 that although the SOC estimation error in the BBDST operating condition followed the pulse change sharply, the maximum error still did not exceed 4%. It could be considered that this design meets the requirements (error ≤ 5%).

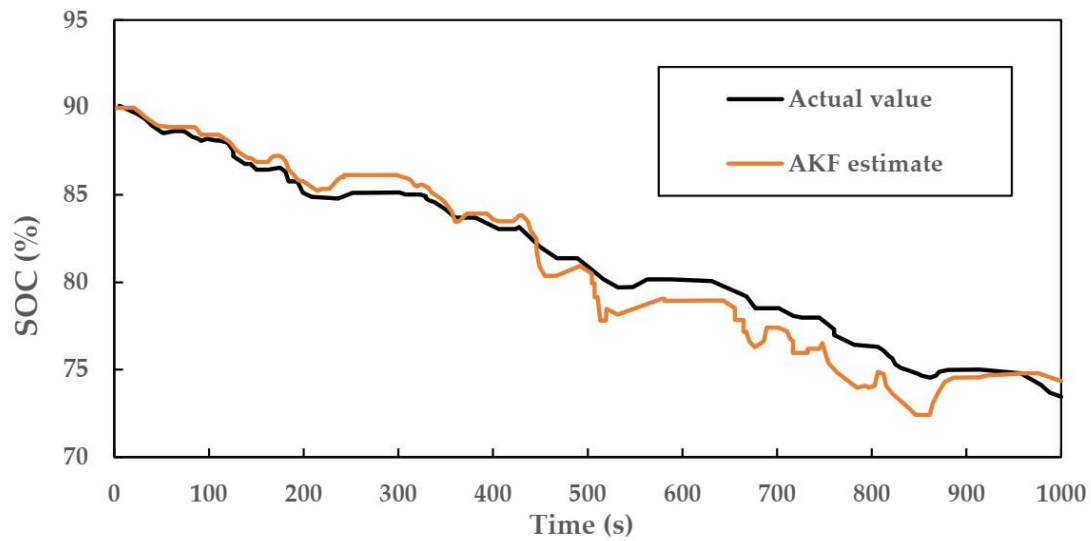


Figure 7. Difference between the SOC estimated value and the actual value under BBDST working conditions.

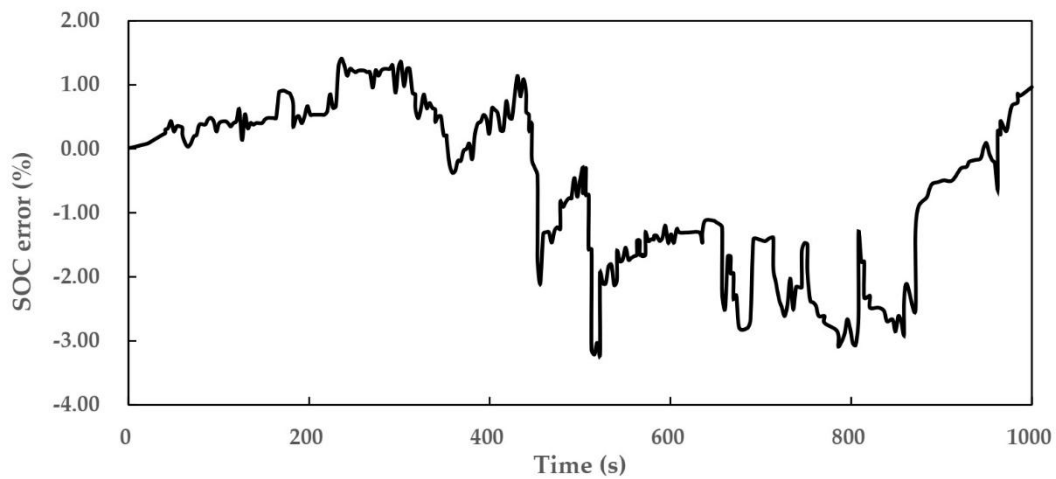


Figure 8. Error between the SOC estimated value and the actual value under BBDST operating conditions.

In actual use, computation time and calculation accuracy are equally important. The calculation time for various SOC estimation algorithms [7,9,17] was performed in MATLAB 2014b (The MathWorks, Natick, Massachusetts, USA) on a PC equipped with an Intel Core i5-8300H CPU @ 2.3 GHz and 8 GB RAM. Table 3 listed the calculation results under BBDST in the entire SOC area (0–100%). It can be seen that the calculation time of the proposed algorithm was relatively small and the accuracy was relatively high. Therefore, the proposed algorithm improved the estimation accuracy without increasing the complexity, which was very suitable for the actual use of EVs.

Table 3. Computing time (s) and error of various SOC estimation algorithms.

Estimation Algorithms	Maximum Absolute Error	Time (s)
Ampere-hour	9.49%	5.951
Two RC KF	3.46%	67.326
Fuzzy control	3.43%	69.542
Proposed algorithm	3.47%	55.756

4.5. Discussion

It can be seen from the experimental results in Sections 4.2–4.4 that the battery SOC estimation algorithm proposed in this paper is accurate and has a short calculation time with good robustness.

However, there are still problems that need to be solved. The error at the beginning of each measurement will be larger. As the experiment progresses, the error value will gradually decrease and tend to be stable. This is suspected to be caused by the polarization of the battery. When the current passes through the battery, battery potential is deviated from the equilibrium potential, which affects the SOC estimation accuracy of the battery. This proves that there is still room for improvement in the algorithm.

Two points will be focused in our future work. Temperature plays a key role in battery characteristics. In order to eliminate the effect of temperature on the results, the battery was placed in the thermostat to maintain a constant temperature (25 °C). However, in electric vehicles, the batteries are not placed in the thermostat and the influence of temperature on the batteries needs to be considered. In the future, it is necessary to further consider the robustness of the SOC estimation algorithm against temperature. Moreover, this paper focused on the performance of the algorithm when the battery was discharged and did not discuss the condition when the battery was charged. In the future, we will study the performance of the estimation algorithm under charge, which may increase the precision with time.

5. Conclusions

In this paper, an adaptive Kalman filter method based on the equivalent circuit model is proposed for the SOC estimation algorithm of a lithium-ion battery. In the adaptive Kalman filter method, the measured data is employed to estimate the mean and the variance of the noise on-line, and continuously corrects the obtained SOC value according to the estimation result. Based on the experimental results, it is not difficult to see that the accuracy of this algorithm is much higher than that of the Kalman filter method, and it has a quick correction effect on the error of the initial value of the SOC, which is extremely suitable for the SOC estimation of the battery online. Moreover, experiments under the BBDST condition prove that this algorithm is suitable for practical applications.

The method proposed in this paper has been proved to be a reasonable, accurate, and realistic SOC estimation method, but there is still room for improvement. Further works include: (1) verification of the application concerning the SOC estimation algorithm based on the equivalent circuit-based adaptive Kalman filter method in the actual BMS; (2) the accuracy of the AKF method for estimating the battery SOC requires the establishment of accurate battery models, but the current battery models are too complicated and the computational cost is high. Therefore, finding a more accurate and uncomplicated battery model will be our next target; and (3) verification of the influence of battery aging on the accuracy of the adaptive Kalman filter.

Author Contributions: All authors contributed to the paper. Conceptualization: X.M. and Q.T.; data curation: Q.T. and X.M.; investigation: X.M. and D.Q.; methodology: X.M.; project administration: D.Z. and D.Q.; software: X.M.; validation: X.M. and D.Z.; writing—original draft: X.M.; writing—review and editing: X.M. and D.Q.

Funding: This work was supported by the National Key R and D Program of China under grant 2017YFB0502700, the National Natural Science Foundation of China (no. 61471195), and the Fundamental Research Funds for the Central Universities (nos. NZ2016105, NJ20150017, NS2014040, and KFJJ20180404), partially by the National Defense Pre-Research Foundation of China (no. 6140413020116HK02001).

Acknowledgments: Xiao Ma and Qing Tao would like to thank Nanjing University of Aeronautics and Astronautics Innovation Base for Postgraduate for the financing of this work and Key Laboratory of Radar Imaging and Microwave Photonics for the equipment of this work.

Conflicts of Interest: The authors declare no conflict of interest.

References

1. Scrosati, B.; Garche, J. Lithium batteries: Status, prospects and future. *J. Power Sources* **2010**, *195*, 2419–2430. [[CrossRef](#)]
2. Capasso, C.; Veneri, O. Experimental analysis on the performance of lithium-based batteries for road full electric and hybrid vehicles. *Appl. Energy* **2014**, *136*, 921–930. [[CrossRef](#)]
3. Abada, S.; Marlair, G.; Lecocq, A.; Petit, M.; Sauvant-Moynot, V.; Huet, F. Safety focused modeling of lithium-ion batteries: A review. *J. Power Sources* **2016**, *306*, 178–192. [[CrossRef](#)]

4. Fleischhammer, M.; Waldmann, T.; Bisle, G.; Hogg, B.-I.; Wohlfahrt-Mehrens, M. Interaction of cyclic ageing at high-rate and low temperatures and safety in lithium-ion batteries. *J. Power Sources* **2015**, *274*, 432–439. [[CrossRef](#)]
5. Perea, A.; Paoletta, A.; Dube, J.; Champagne, D.; Mauger, A.; Zaghbi, K. State of charge influence on thermal reactions and abuse tests in commercial lithium-ion cells. *J. Power Sources* **2018**, *399*, 392–397. [[CrossRef](#)]
6. Liu, D.T.; Li, L.; Song, Y.C.; Wu, L.F.; Peng, Y. Hybrid State of Charge Estimation for Lithium-Ion Battery under Dynamic Operating Conditions. *Int. J. Electr. Power Energy Syst.* **2019**, *110*, 48–61. [[CrossRef](#)]
7. Chen, Y.J.; Yang, G.; Liu, X.; He, Z.C. A Time-Efficient and Accurate Open Circuit Voltage Estimation Method for Lithium-Ion Batteries. *Energies* **2019**, *12*, 1803. [[CrossRef](#)]
8. Feng, F.; Lu, R.; Zhu, C. A Combined State of Charge Estimation Method for Lithium-Ion Batteries Used in a Wide Ambient Temperature Range. *Energies* **2014**, *7*, 3004–3032. [[CrossRef](#)]
9. Liu, Z.; Li, Z.; Zhang, J.; Su, L.; Ge, H. Accurate and Efficient Estimation of Lithium-Ion Battery State of Charge with Alternate Adaptive Extended Kalman Filter and Ampere-Hour Counting Methods. *Energies* **2019**, *12*, 757. [[CrossRef](#)]
10. Khumprong, P.; Yodo, N. A Data-Driven Predictive Prognostic Model for Lithium-Ion Batteries based on a Deep Learning Algorithm. *Energies* **2019**, *12*, 660. [[CrossRef](#)]
11. Waag, W.; Fleischer, C.; Sauer, D.U. Critical review of the methods for monitoring of lithium-ion batteries in electric and hybrid vehicles. *J. Power Sources* **2014**, *258*, 321–339. [[CrossRef](#)]
12. Li, C.; Xiao, F.; Fan, Y. An Approach to State of Charge Estimation of Lithium-Ion Batteries Based on Recurrent Neural Networks with Gated Recurrent Unit. *Energies* **2019**, *12*, 1592. [[CrossRef](#)]
13. Christian, C.; Thomas, H.; Stephen, K.; Andreas, J. A comparative study and review of different Kalman filters by applying an enhanced validation method. *J. Energy Storage* **2016**, *8*, 142–159.
14. Hou, J.; Yang, Y.; He, H.; Gao, T. Adaptive Dual Extended Kalman Filter Based on Variational Bayesian Approximation for Joint Estimation of Lithium-Ion Battery State of Charge and Model Parameters. *Appl. Sci.* **2019**, *9*, 1726. [[CrossRef](#)]
15. Sun, Q.; Zhang, H.; Zhang, J.; Ma, W. Adaptive Unscented Kalman Filter with Correntropy Loss for Robust State of Charge Estimation of Lithium-Ion Battery. *Energies* **2018**, *11*, 3123. [[CrossRef](#)]
16. Hou, J.; He, H.; Yang, Y.; Gao, T.; Zhang, Y. A Variational Bayesian and Huber-Based Robust Square Root Cubature Kalman Filter for Lithium-Ion Battery State of Charge Estimation. *Energies* **2019**, *12*, 1717. [[CrossRef](#)]
17. Liu, X.; Qiao, D.D.; Zheng, Y.J.; Zhou, L. A fuzzy state-of-charge estimation algorithm combining Ampere-Hour and an extended Kalman filter for Li-ion Battery based on multi-model global identification. *Appl. Sci.* **2018**, *8*, 2028. [[CrossRef](#)]
18. Yu, Q.Q.; Xiong, R.; Wang, L.Y.; Lin, C. A comparative study on open circuit voltage models for lithium-ion batteries. *Chin. J. Mech. Eng.* **2018**, *31*, 65–73. [[CrossRef](#)]
19. Sun, D.; Xu, S.; Li, C.; Ji, A.F. Review of state of charge estimation method for Li-ion battery. *Battery Bimonthly* **2018**, *48*, 284–287.
20. Li, Z.; Huang, J.; Liaw, B.Y.; Zhang, J. On state-of-charge determination for lithium-ion batteries. *J. Power Sources* **2017**, *348*, 281–301. [[CrossRef](#)]
21. Plett, G.L. Extended Kalman filtering for battery management systems of LiPB-based HEV battery packs: Part 2. Modeling and identification. *J. Power Sources* **2004**, *134*, 262–276. [[CrossRef](#)]
22. Suleman, A.S.; Dennis, D. Rapid test and non-linear model characterization of solid-state lithium-ion batteries. *J. Power Sources* **2004**, *130*, 266–274.
23. Meng, J.H.; Luo, G.Z.; Mattia, R.; Maciej, S. Overview of lithium-ion battery modeling methods for state-of-charge estimation in electrical vehicles. *Appl. Sci.* **2018**, *659*, 1–17. [[CrossRef](#)]
24. Ning, J.Q.; Zhang, L.P. Method for Determining SOC-OCV Curve of Lithium Battery. China Patent No. CN104297690A, 21 January 2015.
25. Wu, B.; Chen, B. Study the performance of battery models for hybrid electric vehicles. In Proceedings of the 2014 IEEE/ASME 10th International Conference on Mechatronic and Embedded Systems and Applications (MESA), Senigallia, Italy, 10–12 September 2014; pp. 1–6.
26. Rael, S.; Urbain, M.; Renaudineau, H. A mathematical lithium-ion battery model implemented in an electrical engineering simulation software. In Proceedings of the 2014 IEEE 23rd International Symposium on Industrial Electronics (ISIE), Istanbul, Turkey, 1–4 June 2014; pp. 1760–1765.

27. Hu, X.; Li, S.; Peng, H. A comparative study of equivalent circuit models for Li-ion batteries. *J. Power Sources* **2012**, *198*, 359–367. [[CrossRef](#)]
28. Lai, X.; Zheng, Y.J.; Sun, T. A comparative study of different equivalent circuit models for estimating state-of-charge of lithium-ion batteries. *Electrochim. Acta* **2018**, *259*, 566–577. [[CrossRef](#)]
29. Farmann, A.; Sauer, D.U. Comparative study of reduced order equivalent circuit models for on-board state-of-available-power prediction of lithium-ion batteries in electric vehicles. *Appl. Energy* **2018**, *225*, 1102–1122. [[CrossRef](#)]
30. Zhang, C.; Yan, F.W.; Du, C.Q.; Giorgio, R. An improved model-based self-adaptive filter for online state-of-charge estimation of Li-ion batteries. *Appl. Sci.* **2018**, *8*, 2084. [[CrossRef](#)]
31. Christopherson, J.P. *Battery Test Manual for Electric Vehicles*; Idaho National Laboratory: Idaho Falls, ID, USA, 2015.
32. Ouyang, M.G.; Liu, G.M.; Lu, L.G.; Li, J.Q.; Han, X.B. Enhancing the estimation accuracy in low state-of-charge area: A novel onboard battery model through surface state of charge determination. *J. Power Sources* **2014**, *270*, 221–237. [[CrossRef](#)]
33. Lai, X.; Zheng, Y.J.; Zhou, L.; Gao, W.K. Electrical behavior of overdischarge-induced internal short circuit in lithium-ion cells. *Electrochim. Acta* **2018**, *278*, 245–254. [[CrossRef](#)]
34. Panchal, S.; Rashid, M.; Long, F.; Mathew, M.; Fraser, R.; Fowler, M. Degradation testing and modeling of 200 ah LiFePO₄ battery. In Proceedings of the WCX World Congress Experience, Detroit, MI, USA, 10–12 April 2018. SAE Technical Paper.
35. Wang, L.M.; Lu, D.; Liu, Q.; Liu, L.; Zhao, X.L. State of charge estimation for LiFePO₄ battery via dual extended Kalman filter and charging voltage curve. *Electrochim. Acta* **2019**, *296*, 1009–1017. [[CrossRef](#)]
36. Zhang, Z.L.; Cheng, X.; Lu, Z.Y.; Gu, D.J. SOC estimation of lithium-ion batteries with AEKF and wavelet transform matrix. *IEEE Trans. Power Electron.* **2017**, *32*, 7626–7634. [[CrossRef](#)]
37. Lai, X.; Qin, C.; Gao, W.K.; Zheng, Y.J.; Yi, W. A state of charge estimator based extended Kalman filter using an electrochemistry-based equivalent circuit model for lithium-ion batteries. *Appl. Sci.* **2018**, *8*, 1592. [[CrossRef](#)]
38. Wei, J.W.; Dong, G.Z.; Chen, Z.H.; Kang, Y. System state estimation and optimal energy control framework for multicell lithium-ion battery system. *Appl. Energy* **2017**, *187*, 37–49. [[CrossRef](#)]
39. Sun, F.C.; Meng, X.F.; Lin, C.; Wang, Z.P. Dynamic stress test profile of power battery for electric vehicle. *Trans. Beijing Inst. Technol.* **2010**, *30*, 297–301.



© 2019 by the authors. Licensee MDPI, Basel, Switzerland. This article is an open access article distributed under the terms and conditions of the Creative Commons Attribution (CC BY) license (<http://creativecommons.org/licenses/by/4.0/>).